AFRL-ML-WP-TP-2006-507

CORROSION PROPERTIES OF Ca BASED BULK METALLIC GLASSES (PREPRINT)

James Dahlman, O.N. Senkov, J.M. Scott, and D.B. Miracle

OCTOBER 2006

Approved for public release; distribution is unlimited.

STINFO COPY

MATERIALS AND MANUFACTURING DIRECTORATE
AIR FORCE RESEARCH LABORATORY
AIR FORCE MATERIEL COMMAND
WRIGHT-PATTERSON AIR FORCE BASE, OH 45433-7750

REPORT DOCUMENTATION PAGE

Form Approved
OMB No. 0704-0188

1. REPORT DATE *(DD-MM-YY)*	2. REPORT TYPE	3. DATES COVERED *(From - To)*
October 2006	Conference Paper Preprint	

4. TITLE AND SUBTITLE
CORROSION PROPERTIES OF Ca BASED BULK METALLIC GLASSES (PREPRINT)

5a. CONTRACT NUMBER
FA8650-04-D-5233

5b. GRANT NUMBER

5c. PROGRAM ELEMENT NUMBER
62102F

6. AUTHOR(S)
James Dahlman (SOCHE)
O.N. Senkov and J.M. Scott (UES, Inc.)
D.B. Miracle (AFRL/MLLM)

5d. PROJECT NUMBER
2311

5e. TASK NUMBER
00

5f. WORK UNIT NUMBER
02

7. PERFORMING ORGANIZATION NAME(S) AND ADDRESS(ES)

SOCHE
3155 Research Blvd., Suite 204
Dayton, OH 45420

UES, Inc.
4401 Dayton-Xenia Road
Dayton, OH 45432

Metals Branch (AFRL/MLLM)
Metals, Ceramics, and Nondestructive Evaluation Division
Materials and Manufacturing Directorate
Air Force Research Laboratory
Air Force Materiel Command
Wright-Patterson Air Force Base, OH 45433-7750

8. PERFORMING ORGANIZATION REPORT NUMBER

9. SPONSORING/MONITORING AGENCY NAME(S) AND ADDRESS(ES)
Materials and Manufacturing Directorate
Air Force Research Laboratory
Air Force Materiel Command
Wright-Patterson AFB, OH 45433-7750

10. SPONSORING/MONITORING AGENCY ACRONYM(S)
AFRL-ML-WP

11. SPONSORING/MONITORING AGENCY REPORT NUMBER(S)
AFRL-ML-WP-TP-2006-507

12. DISTRIBUTION/AVAILABILITY STATEMENT
Approved for public release; distribution is unlimited.

13. SUPPLEMENTARY NOTES
Conference paper submitted to the 2006 Proceedings of the Fifth International Bulk Metallic Glasses Conference, to be published in a special issue of the journal, Materials Transactions, published by the Japan Institute of Metals.

The U.S. Government is joint author of this work and has the right to use, modify, reproduce, release, perform, display, or disclose the work. This paper contains color. PAO Case Number: AFRL/WS 06-2302; date cleared: 27 Sep 2006.

14. ABSTRACT
The corrosion properties of ternary ($Ca_{65}Mg_{15}Zn_{20}$ and $Ca_{50}Mg_{20}Cu_{30}$), quaternary ($Ca_{55}Mg_{18}Zn_{11}Cu_{16}$), and quinternary ($Ca_{55}Mg_{15}Al_{10}Zn_{15}Cu_5$) amorphous alloys were evaluated using static environment aqueous submersion (SEAS) at room temperature. Ca-Mg-Zn and Ca-Mg-Cu alloy systems underwent destructive corrosion reactions. Ca-Mg-Zn-Cu and Ca-Mg-Zn-Cu-Al based amorphous alloys demonstrated positive corrosion properties, forming thick corrosion layers up to 40 μm thick in the quaternary alloys and 20 μm thick in the quinternary compositions. Corrosion products were evaluated using X-ray diffraction (XRD), X-ray Fluorescence (XRF), Scanning Electron Microscopy (SEM), and Electron Dispersion Spectroscopy (EDS).

15. SUBJECT TERMS
Metallic Glass, Corrosion, Calcium Alloy

16. SECURITY CLASSIFICATION OF:			17. LIMITATION OF ABSTRACT:	18. NUMBER OF PAGES	19a. NAME OF RESPONSIBLE PERSON (Monitor)
a. REPORT	b. ABSTRACT	c. THIS PAGE			D.B. Miracle
Unclassified	Unclassified	Unclassified	SAR	28	19b. TELEPHONE NUMBER *(Include Area Code)* N/A

Standard Form 298 (Rev. 8-98)
Prescribed by ANSI Std. Z39-18

Corrosion Properties of Ca Based Bulk Metallic Glasses

James Dahlman[a,c], O.N. Senkov[a,b], J.M. Scott[a,b], D.B. Miracle[a]

[a]Air Force Research Laboratory, Materials and Manufacturing Directorate, Wright Patterson AFB, OH, 45433, USA

[b]UES, Inc., Materials and Processes Division, 4401 Dayton-Xenia Road, Dayton, OH, 45432, USA

[c]SOCHE, Student Research Program, 3155 Research Blvd., Suite 204, Dayton, OH, 45420, USA

Available 1 October 2006

Abstract

The corrosion properties of ternary ($Ca_{65}Mg_{15}Zn_{20}$ and $Ca_{50}Mg_{20}Cu_{30}$), quaternary ($Ca_{55}Mg_{18}Zn_{11}Cu_{16}$), and quinternary ($Ca_{55}Mg_{15}Al_{10}Zn_{15}Cu_5$) amorphous alloys were evaluated using static environment aqueous submersion (SEAS) at room temperature. Ca-Mg-Zn and Ca-Mg-Cu alloy systems underwent destructive corrosion reactions. Ca-Mg-Zn-Cu and Ca-Mg-Zn-Cu-Al based amorphous alloys demonstrated positive corrosion properties, forming thick corrosion layers up to 40 μm thick in the quaternary alloys and 20 μm thick in the quinternary compositions. Corrosion products were evaluated using X-ray diffraction (XRD), X-ray Fluorescence (XRF), Scanning Electron Microscopy (SEM), and Electron Dispersion Spectroscopy (EDS).

Keywords: Metallic Glass, Corrosion, Calcium Alloy

Introduction

Bulk amorphous metals are attractive materials for several reasons. An absence of microstructural features such as crystal plains, dislocations, grain and phase boundaries contribute to appealing mechanical properties such as high hardness and high specific strength. The amorphous structure also results in attractive magnetic properties such as high magnetic permeability. Corrosion studies have also established amorphous metals as a group of materials with corrosion properties much more desirable than their crystalline counterparts. As a result, metallic glasses have found their way into common applications including golf club heads, magnetic security strips, step-down transformers and cell phone cases. Within the last 15 years, many successful steps have been made in both understanding the properties of amorphous metals and in processing bulk quantities efficiently.

Calcium based bulk metallic glasses constitute a new class of amorphous materials. The first successful synthesis of Ca-based bulk metallic glasses (CaBMGs) produced $Ca_{57}Mg_{19}Cu_{24}$ and $Ca_{60}Mg_{20}Ag_{20}$ in amorphous cylinders with diameters up to 4 mm [1] and $Ca_{60}Mg_{20}Ag_{10}Cu_{10}$ with a maximum diameter of 7 mm [2]. Since then, additional work has provided specific criteria for selecting CaBMG compositions [3-6] and a number of CaBMG's have been produced in Ca-Mg-Zn [7-11], Ca-Mg-Cu [11,12], Ca-Mg-Al [4,13] and other systems [4,13], . Significant interest and development in this material has been catalyzed by properties that include densities approaching ~2.0 g/cm^3 and a low Young's modulus, near 20-35 GPa [14,15]. However, crystalline Ca is extremely reactive, and studies evaluating the corrosion resistance of amorphous Ca-based alloys are required to explore what may be a limiting factor for practical applications of CaBMGs [16].

The purpose of this report is to describe the stability of Ca BMGs in a static aqueous environment. The results from two ternary alloys ($Ca_{65}Mg_{15}Zn_{20}$), ($Ca_{50}Mg_{20}Cu_{30}$), one quaternary alloy ($Ca_{55}Mg_{18}Zn_{11}Cu_{16}$) and one quinternary alloy ($Ca_{55}Mg_{15}Al_{10}Zn_{15}Cu_{5}$) will be discussed. A uniform procedure for preparing CaBMGs for corrosion analysis is developed and described. The discourse will assess the change in mass of each sample and attempt to identify the experimental reaction byproducts. The results of these experiments will help guide further development of CaBMG corrosion resistance so that applications may take advantage of their attractive properties. Finally, a correlation between the chemical composition and the corrosion resistance of CaBMGs will be identified.

Experimental Procedures

Four alloys were chosen to assess the individual contributions from different alloying additions. Previous work established high glass forming ability (GFA) of Ca-Mg based BMGs [6-12]. Zn and Cu were chosen, both individually and alloyed together, in order to evaluate the corrosion resistance in the Ca-Mg system. Finally, Al was chosen to evaluate the corrosion effect of this protective oxide-forming material. Each composition was prepared with high purity elements (see Table 1). The mass of each individual component was calculated for a 15 g sample, and was weighed to within one-tenth of a milligram. Once measured, the elements were mixed and induction melted in a water-cooled Cu hearth with a diameter of 31.75 mm under a positive pressure argon atmosphere. Once the alloy was successfully produced, it was placed in a desiccation chamber until it was ready to be cast. Total exposure time between melting and placement in the desiccator was limited to less than twenty minutes to minimize possible corrosion reactions between the specimen and the environment.

Approximately 5.0 grams of each alloy were induction re-melted under a positive pressure argon gas in a quartz crucible with a 2 mm hole in the bottom and injected into a water-cooled Cu mold cavity with dimensions of 15 mm ×15 mm × 4 mm. Previous work demonstrated that these alloys have the maximum amorphous thicknesses well beyond 4 mm (see Table 2). Consequently it was assumed that the specimens were thoroughly glassy; although amorphicity of their surface layers was additionally examined by XRD.

To maintain a uniform surface with an easily measured surface area, each sample was first polished on 320 grit SiC paper, then on 600 SiC grit paper with water lubricant until a rectangular prism was produced. The samples were then briefly ground on 600 grit SiC paper without water to remove corrosion products from the surface. Once polishing was complete, each alloy underwent dimensional analysis with a pair of electronic calipers accurate to within ±.01 mm. Less than twenty minutes after polishing, the samples were placed in a desiccator until testing began.

The experiment evaluated the corrosion resistance in a static aqueous environment with a timeframe of ~700 hours. One sample from each alloy was attached to a nylon string and clasp with a mass of 0.1710 g. The sample was then suspended in 150 mL of distilled water (Di-H_20) by attaching the plastic line around a cylindrical piece of wood, and suspending the wood over the opening to a 250 mL beaker. An Al hook system was attached to a scale to measure the sample mass at selected times during the exposure. The sample weight change data points were collected while the sample was in distilled water (See Figure 1).

After ~700 hours of exposure in water, the Ca-Mg-Cu alloy was completely transformed into a spalled corrosion product in the form of powder. After ~2100 hours, the Ca-Mg-Zn alloy also entirely decomposed into powder. These corrosion products were stained with filter paper

for one hour, then heat treated at 100ºC for seventy-two hours in order to remove the water from the powder. An X-ray diffractometer Rigaku Rotaflex, at Cu K_α radiation, was used to identify phases in each respective sample and to evaluate the sample surface amorphicity. A scanning electron microscope (SEM) with an attached energy-dispersive spectrometer (EDS) was used to analyze the microstructure and chemistry of the amorphous samples and corrosion products.

Powdered samples were prepared for SEM analysis by coating with carbon to ensure electrical conductivity across the entire sample. Solid amorphous samples with oxidized surfaces were cross-sectional cut and cold mounted into an epoxy. The surfaces were then mechanically polished, cleaned and the mounts were coated with a carbon layer for conductivity. Any heating during processing was minimized to avoid crystallization. SEM was performed at 15 keV, using both secondary electron and back-scatter electron imaging, and EDS analysis was conducted using an accelerated voltage of 25 kV to ensure data quality.

Results and Discussion

Corrosion and crystallization during the sample surface polishing

While in contact with water during polishing, the Ca-Mg-Zn glassy alloy was very reactive, bubbling violently, but showed an exceptionally low pitting frequency. The other alloys did not corrode as aggressively, but had pitting present over many of the large faces. XRD was performed on 14 samples following the polishing procedure to ensure a fully amorphous sample surface. After dry polishing, without using water or oil, the surface layer of the amorphous samples was partially crystallized and corresponding X-ray diffraction patterns showed intense crystalline peaks (Figure 2a). However, the sample surface remained fully

amorphous if water or oil were used as a coolant and a low polishing pressure was applied during the surface grinding and polishing (Figure 2b). The $Ca_{65}Mg_{15}Zn_{20}$ amorphous samples were most sensitive for crystallization as they had the lowest crystallization temperature of T_x = 137ºC [9], followed by, $Ca_{55}Mg_{15}Al_{10}Zn_{15}Cu_5$ (T_x = 149ºC), $Ca_{55}Mg_{18}Zn_{11}Cu_{16}$ (T_x = 166ºC) [11] and $Ca_{50}Mg_{20}Cu_{30}$ (T_x = 169ºC) [12] amorphous samples.

Corrosion in Water

The four alloys subjected to static aqueous environment underwent corrosive reactions over ~700 hours. $Ca_{65}Mg_{15}Zn_{20}$ and $Ca_{50}Mg_{20}Cu_{30}$ both underwent corrosive reactions resulting in a net loss of mass. A dynamic environmental submersion method serves to alleviate this problem. Early testing also indicates submersion in a DEAS system may increase the rate of reaction between the specimen and the environment, further accelerating the testing procedure. When placed in Di-H_2O, an immediate reaction between the $Ca_{65}Mg_{15}Zn_{20}$ glassy alloy and water took place. The surface area was quickly covered in bubbles stemming from a corrosion reaction. The corrosion reaction between $Ca_{65}Mg_{15}Zn_{20}$ and Di-H_2O led to formation of a non-protective compound on the sample surface, which was spalled and collected at the bottom of the beaker in white and gray powder form (Figure 3). The spalled material blended with the Di-H_2O, creating an opaque environment. These unstable reaction products and the consequent loss in mass establish $Ca_{65}Mg_{15}Zn_{20}$ unsuitable for sustained exposure to aqueous environments.

The time dependence of the weight loss per unit surface area of a $Ca_{65}Mg_{15}Zn_{20}$ amorphous sample during reaction with Di-H_2O is shown in Figure 4. The weight continuously decreases with time and after ~700 hour holding in water, the sample loses about 65% of its mass. The experimental results also indicate (see Figure 4) that the weight loss per unit area, *W*,

can be described by a parabolic dependence on the holding time, *t*, with a rate constant a_1 = -0.064 mg/cm^2/s$^{0.5}$ and b_1 = 0:

$$W = at^{0.5} + b \qquad (1)$$

X-ray analysis of the spalled corrosion powder product from the $Ca_{65}Mg_{15}Zn_{20}$ amorphous sample identified three primary phases, which are Calcium Hydroxide ($Ca(OH)_2$), Calcium Zinc Hydroxide Hydrate ($Ca[Zn(OH)_3]_2 \cdot H_2O$) and Calcium Zinc ($Ca_3Zn$). Supporting the XRD results, X-ray fluorescence of the powder indicated a major concentration of Ca and Zn, with Mg existing in only minor concentrations.

Corrosion behavior of the ternary $Ca_{50}Mg_{20}Cu_{30}$ glassy alloy is illustrated in Figure 5 and it is considerably different from that of $Ca_{65}Mg_{15}Zn_{20}$. During the first 100 hours of water exposure the $Ca_{50}Mg_{20}Cu_{30}$ glassy alloy shows a very minor weight gain due to creating an oxide layer (see Figure5 enclosure). This increase in weight can be described by a parabolic time dependence, Equation (1), with the rate constant $a_2 = 8.2 \times 10^{-4}$ mg/cm^2/s$^{0.5}$ and b_2 = 0. However, after this point, the alloy started to lose weight and black spalled material appeared at the bottom of the beaker. After ~150 hours of the water exposure, the non-protective reaction product and the corrosion layer visible on the specimen changed in color from black to a blend of gold and black, and a rapid decrease in mass was observed. This rapid decrease in the weight, within 150 to 500 hours of holding in water, can be described by Equation (1) with a_3 = -0.162 mg/cm^2/s$^{0.5}$ and b_3 = 140 mg/cm^2. The heavy corrosion reaction was evidenced by a drastic change in amount of the surface area covered by gaseous bubbles. After about 550 hours of exposure, rapid drops in the sample weight occurred leading to entire decomposition of the sample (see Figure 5).

X-ray diffraction of the spalled corrosion product from the $Ca_{50}Mg_{20}Cu_{30}$ amorphous sample showed the presence of two primary phases, Cu_2O and $Ca(OH)_2$, and several minor unidentified phases. X-ray fluorescence (XRF) chemical analysis supports the presence of these two major phases, indicating a strong concentration of Ca and Cu in the spalled corrosion product.

Contrasting the heavy corrosion of the pair of the ternary alloys, both the quaternary alloy ($Ca_{55}Mg_{18}Zn_{11}Cu_{16}$) and the quinternary alloy ($Ca_{55}Mg_{15}Al_{10}Zn_{15}Cu_5$) show much better corrosion behavior, with a steady weight gaining. The quaternary $Ca_{55}Mg_{18}Zn_{11}Cu_{16}$ alloy gained mass at a linear rate for the first 250 hours (Figure 6), and the time dependence of the weight gain can be described by a linear Equation:

$$W = ct+d \qquad (2)$$

where c = 1.45x10^{-4} mg/cm^2/s is the linear oxidation rate and d = 1.36 mg/cm^2/s. Bubbles were present on the blackened specimen throughout the testing. After ~250 hours, a small amount of black spalled material formed on the bottom of the glass beaker. Once the spalled material was observed, the corrosion behavior changed from linear to a parabolic one (Figure 6), which can be described by Equation (1) with a_4 = 2.88x10^{-4} mg/cm^2/s$^{0.5}$ and b_4 = 3.1 mg/cm^2. After ~700 hours, the sample had increased 17.4 milligrams, or 1.636%. This large change in mass was verified by SEM analysis indicating an oxide film with a large thickness, roughly 30 μm thick after corrosion in water for ~2100 hours (Figure 7). The film appeared to consist of three layers, with the majority of the structural defects occurring in the second layer. A bright region at the bottom of this picture represents an image of a non-oxidized sample, above which three oxide layers are seen, which are identified by different gray levels. The first oxide layer, which is adjacent to the non-oxidized sample region, is approximately 3 μm thick and dark. It does not have any visible defects, except small cracks propagated from the second layer. The second,

intermediate, layer is much thicker, about 15 μm, and has a lighter contrast and contains open cracks which are perpendicular to the sample surface. The third, external, layer is also thick and contains cracks, which are parallel to the sample surface; it has the darkest contrast and an uneven external surface. The different contrasts of the oxide layers in the backscatter electron imaging mode indicate different chemistry of these layers; in particular, the darker contrast indicates higher concentration of lighter elements. EDS analysis of the oxide layers indicate a very large presence of Ca, Mg and O in the outermost layer. This analysis also indicates that the first thin oxide layer mainly contains Ca, Zn and O, while the middle layer contains an increased concentration of Cu, Ca and O.

The $Ca_{55}Mg_{15}Al_{10}Zn_{15}Cu_5$ amorphous alloy developed a very stable oxide layer during water exposure. Bubbles indicating the presence of a reaction were however present throughout the experiment. The oxidation followed by a parabolic dependence on the oxidation time after some period of instability at the beginning of the experiment (Figure 8). During the stable regime, the weight gain can be described by Equation (1), with the parabolic rate $a_5 = 2.15 \times 10^{-4}$ $mg/cm^2/s^{0.5}$ and $b_5 = 0.35$ mg/cm^2. After holding in water for ~ 2100 hours, this amorphous alloy became very fragile and required careful handling to avoid braking apart.

SEM analysis of the $Ca_{55}Mg_{15}Al_{10}Zn_{15}Cu_5$ amorphous alloy showed a double oxide layer. The first oxide layer, adjacent to the substrate, had an even thickness of about 10-20 μm along the entirety of the sample (Figure 9a). Cracks perpetrated this oxide layer frequently, and cracks were present throughout the substrate (Figure 9b). These cracks help explain high fragility of the specimen after the water corrosion testing. Finally, large globular mounds up to 100 μm thick were found attached to the first oxide layer (Figure 9c). EDS showed the mounds to have a

different chemical composition than the first oxide layer, with large amounts of Ca, Mg, Zn, and O in the globular formation. The same analysis indicated a strong presence of Ca, Mg, Zn, Cu, O and Al in the first oxide layer.

Conclusions

Preparing the Ca-based amorphous samples effectively allows for an even testing surface on a 15 mm x 15 mm x 4 mm sample after roughly two hours. The procedure should involve cutting the sample with low pressure and low saw speed, and soft polishing with oil-based coolant to avoid crystallization. Exposure to air should also be limited between steps. Using these techniques, quantitative data can be collected fairly quickly with a SEAS procedure. However, SEAS testing should be used with caution, as contamination of the environment may cause secondary reactions and erratic behavior.

Ca-Mg-Zn and Ca-Mg-Cu bulk amorphous alloys demonstrate good glass forming ability and relatively low densities, but poor corrosion properties. During holding in water, the $Ca_{65}Mg_{15}Zn_{20}$ alloy decomposes into a multiphase powder, with the three primary phases; $Ca(OH)_2$, Ca_3Zn and $Ca[Zn(OH)_3]_2 \cdot H_20$.

The $Ca_{50}Mg_{20}Cu_{30}$ amorphous alloy, during holding in water for the first 100 hours, appears to be stable and shows a very small increase in weight due to formation of a hydroxide layer. However, it decomposes rapidly into two major phases; Cu_2O and $Ca(OH)_2$, during following 400 hours.

The $Ca_{55}Mg_{18}Zn_{11}Cu_{16}$ amorphous alloy is rather corrosion resistant in the aqueous environment. It gains mass due to oxidation at a linear rate for the first 250 h and at a parabolic rate after that. The oxide film consists of 3 distinctive layers and, after ~2100 h exposure in water, it is ~ 40 μm thick, contributing to a gain in mass of 1.64%. However, the outermost

oxide layer is subject to spallation. For this reason, further studies over longer time intervals should be included in order to evaluate the long-term stability of the oxide layer in this glassy alloy.

Adding Al to form the $Ca_{55}Mg_{15}Al_{10}Zn_{15}Cu_5$ bulk amorphousalloy enhances the stability of the oxide layer, which remains up to 30 μm thick, and increases oxidation resistance. Adding Al also decreases the density of the alloy, making it very attractive for lightweight structures. However, after long time exposure in water this alloy becomes very fragile and brakes easily under small finger pressure.

Acknowledgements

Discussions with Dr. Nathan Klingbeil and William Rillo are greatly appreciated. Support for this research was provided by the United State Air Force Research Laboratory, on-site contract No. FA8650-04-D-5233.

References

1. K. Amiya and A. Inoue. Mater. Trans., 43 (2002) 81-84.
2. K. Amiya and A. Inoue. Mater. Trans., 43 (2002) 2578-2581.
3. O.N. Senkov and J.M. Scott, *MRS Proceedings, Vol. 806,* Mater. Res. Soc., Warrendale, PA, 2003, pp. 145-150.
4. O.N. Senkov and J.M. Scott, *Scripta Mater.,* 50 (2004) 449-452.
5. O.N. Senkov, D.B. Miracle, and H.M. Mullens, *J. Applied Physics*, 97 (2005) 103502-1-7.
6. S. Gorsse, G. Orveillon, O.N. Senkov, D.B. Miracle, *Phys. Rev. B,* 73 (2006) 224202.
7. O.N. Senkov, J.M. Scott, *Materials Letters*, 58 (2004,) 1375-1378.
8. E.S. Park, D.H. Kim, J. Mater. Res. 19 (2004) 685-688.
9. O.N. Senkov, J.M. Scott, J. Non-Cryst. Solids, 351 (2005) 3087-3094.
10. E.S. Park, W.T. Kim, D.H. Kim, Mater. Sci. Forum, 475-479 (2005) 3415-3418.
11. O.N. Senkov, D.B. Miracle, J.M. Scott, Intermetallics, 14 (2006) 1055-1060.
12. O.N. Senkov, J.M. Scott, D.B. Miracle, J. Alloys & Comp. 324 (2006).
13. F.Q. Guo, S.J. Poon, G.J. Shiflet, Appl. Phys. Letters, 84 (2004) 37-39.
14. Z. Zhang, V. Keppens, O.N. Senkov, D.B. Miracle, Mater. Sci. Eng. A (2006).
15. V. Keppens, Z. Zhang, O. N. Senkov, and D. B. Miracle, Phil. Mag. (2006).
16. M.L. Morrison, R.A. Buchanan, O.N. Senkov, D.B. Miracle, P.K. Liaw, *Metall. Mater. Trans. A*, 37 (2006) 1239-1245.

TABLES

Table 1 Purity of elemental constituents

Element	Ca	Mg	Zn	Cu	Al
Purity	99.5000%	99.9800%	99.9900%	99.9999%	99.9000%

Table 2. Alloy compositions sought to evaluate differences in corrosion resistance with different elements.

Composition (Atomic %)	$Ca_{55}Mg_{18}Zn_{11}Cu_{16}$	$Ca_{65}Mg_{15}Zn_{20}$	$Ca_{50}Mg_{20}Cu_{30}$	$Ca_{55}Mg_{15}Al_{10}Zn_{15}Cu_{5}$^
Composition Wt.%	$Ca_{50}Mg_{10}Zn_{16}Cu_{23}$	$Ca_{61}Mg_{8}Zn_{31}$	$Ca_{46}Mg_{11}Cu_{43}$	$Ca_{53}Mg_{9}Al_{6}Zn_{24}Cu_{8}$
Theoretical Density* (g/cm^3)	2.31	2.05	2.45	2.16
Maximum amorphous Thickness (mm)	>10.0	6.0	8.0	6.0

*Theoretical density was calculated using the following equation:

$$\rho = \frac{100}{\sum_{i=1}^{n} \left(\frac{Wt.\%}{\rho} \right)_i}$$

^ The alloy was first reported by Guo, Poon and Shiflet at DARPA SAM1 in 2005.

Figures

Figure 1. Experimental setup involved massing samples suspended in a distilled static aqueous environment.

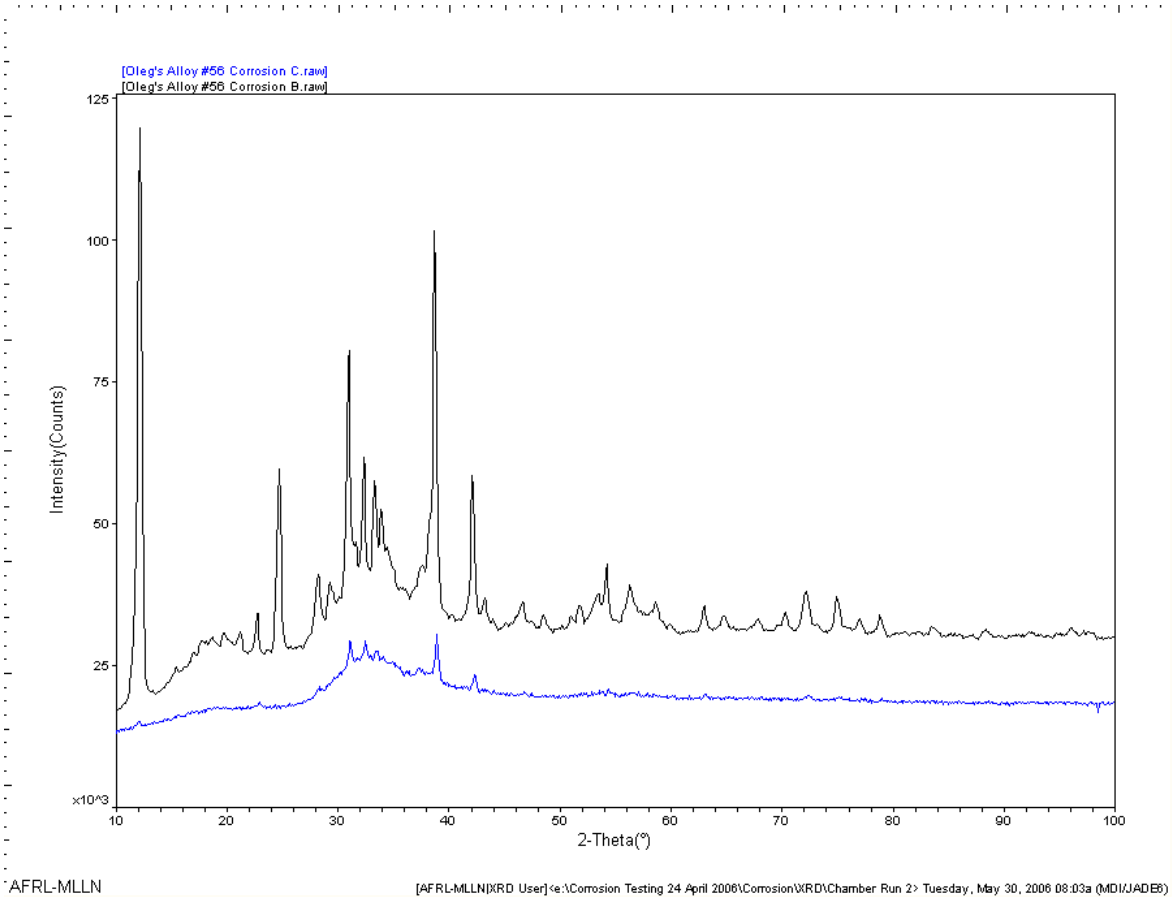

Figure 2. X-ray diffraction patterns of $Ca_{65}Mg_{15}Zn_{20}$ amorphous plates after (a) dry grinding and polishing and (b) grinding and polishing with cooling water and oil. A broad 2θ is seen in figure (b), indicating amorphicity at the surface of the sample polished with low pressure and low heat.

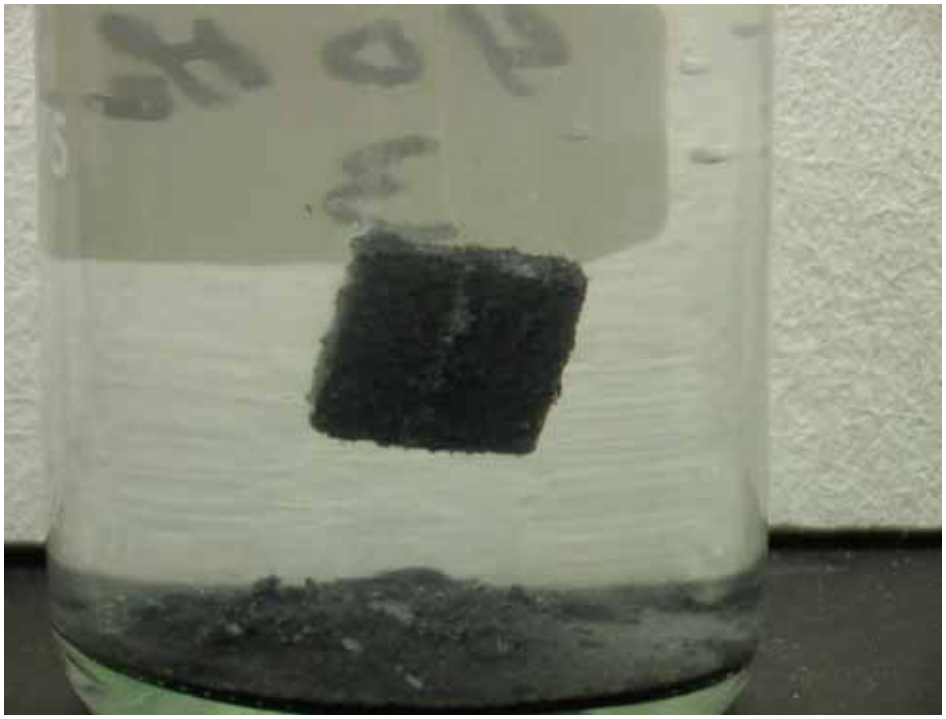

Figure 3. A corroded Ca-Mg-Zn sample with a corrosion product and gas bubbles on its surface and spalled material on the bottom of a beaker.

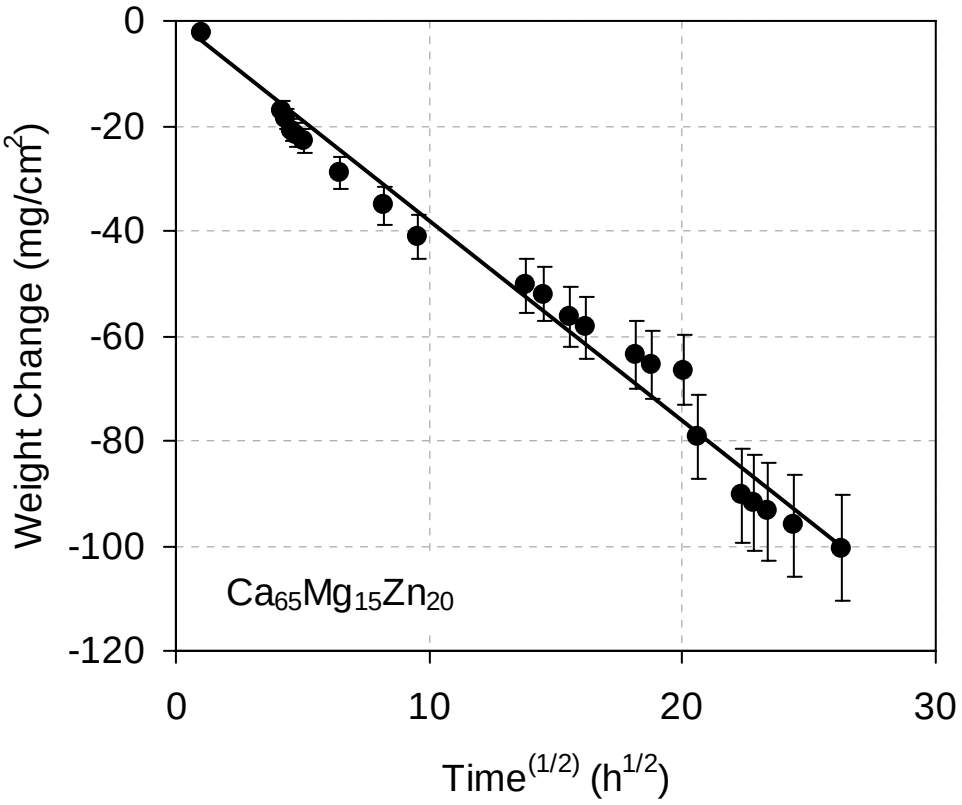

Figure 4. Weight change per unit surface area of a ternary $Ca_{65}Mg_{15}Zn_{20}$ metal glass versus square root of holding time in water. The weight loss can be fit by a parabolic time dependence, $W_1 = -a_1 t^{0.5}$, where a_1 = 0.064 mg/(cm^{2}s$^{0.5}$) is a rate constant.

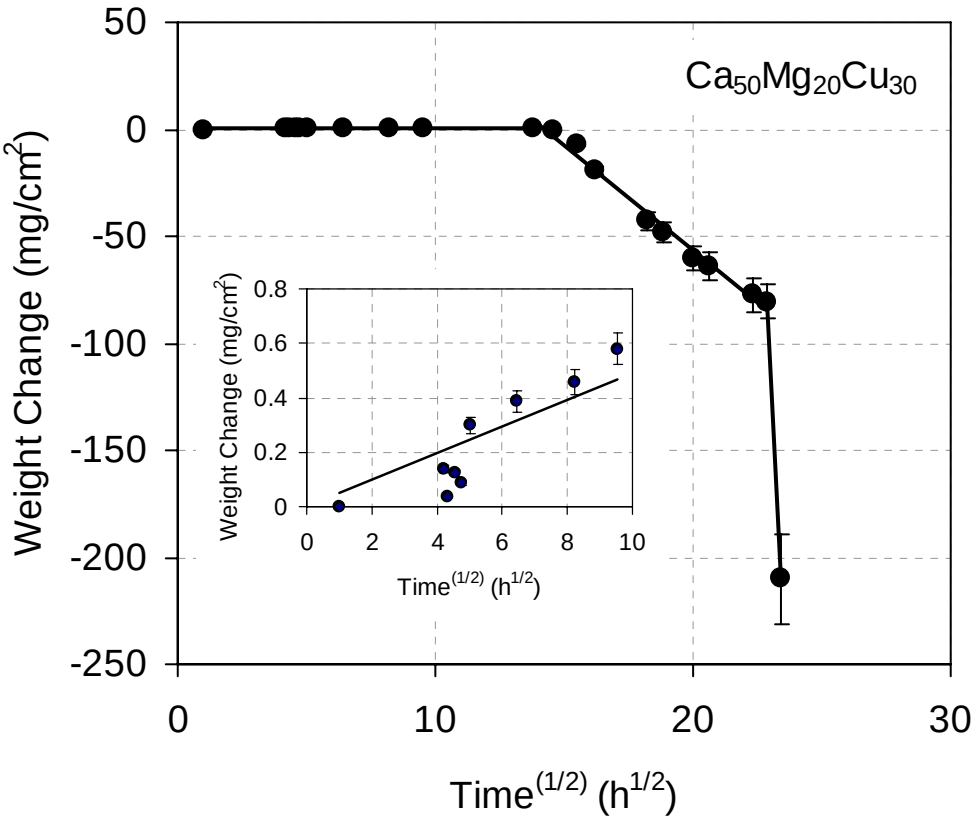

Figure 5. Weight change per unit surface area of a ternary $Ca_{50}Mg_{20}Cu_{30}$ metal glass versus square root of holding time in water. An insert shows behavior during the first 100 hours of holding in water.

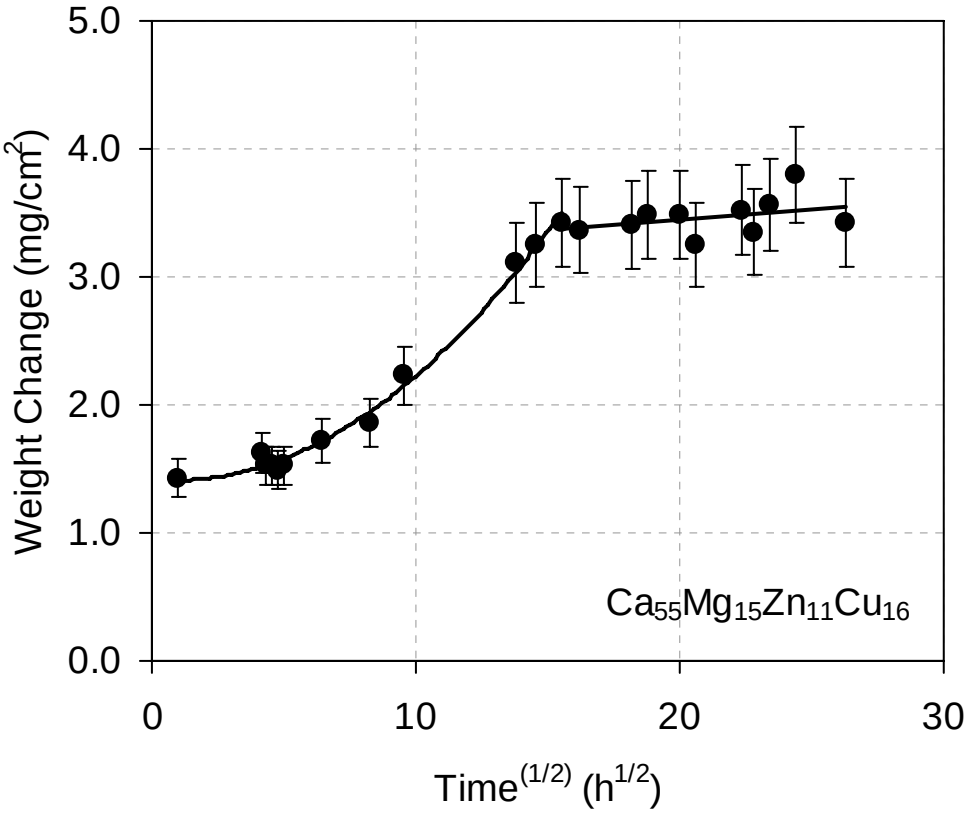

Figure 6. Weight change per unit surface area of a $Ca_{55}Mg_{15}Zn_{11}Cu_{16}$ metal glass versus square root of holding time in water.

Figure 7. SEM backscatter image of a near surface region of a $Ca_{55}Mg_{18}Zn_{11}Cu_{16}$ amorphous sample after corrosion in water for 2100 hours. A bright region at the bottom represents an image of a non-oxidized sample, above which three oxide layers are seen, which are identified by different gray levels. The darkest layer signifies the epoxy in which the sample was set.

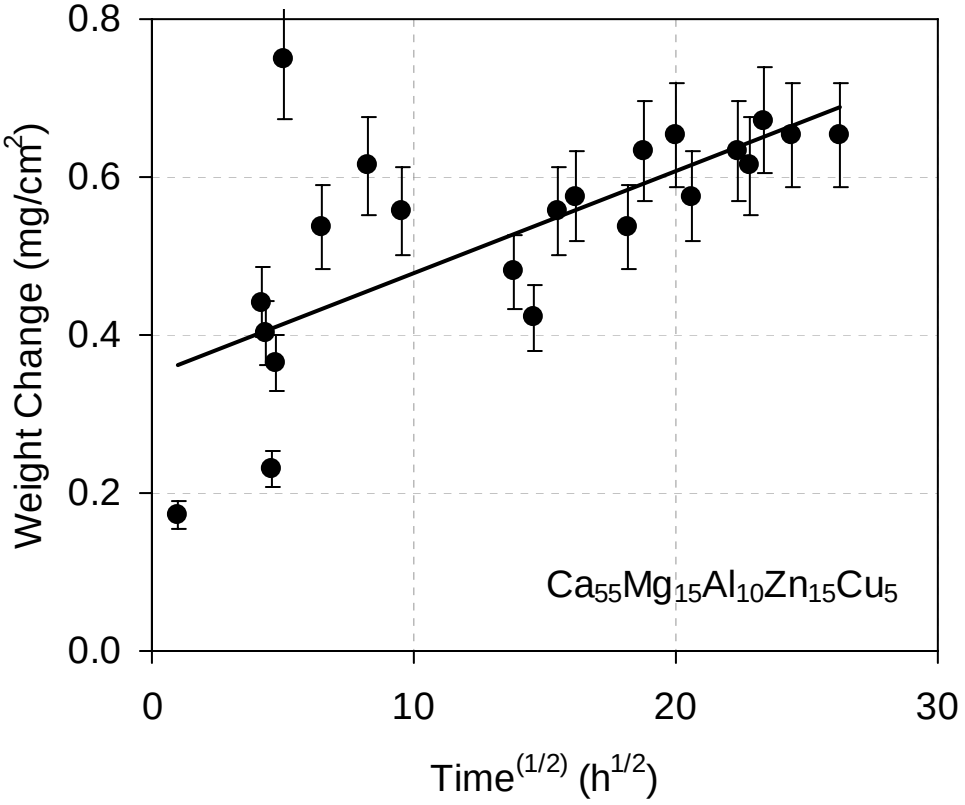

Figure 8. Weight change per unit surface area of a $Ca_{55}Mg_{15}Al_{10}Zn_{15}Cu_5$ metal glass versus square root of holding time in water.

(a)

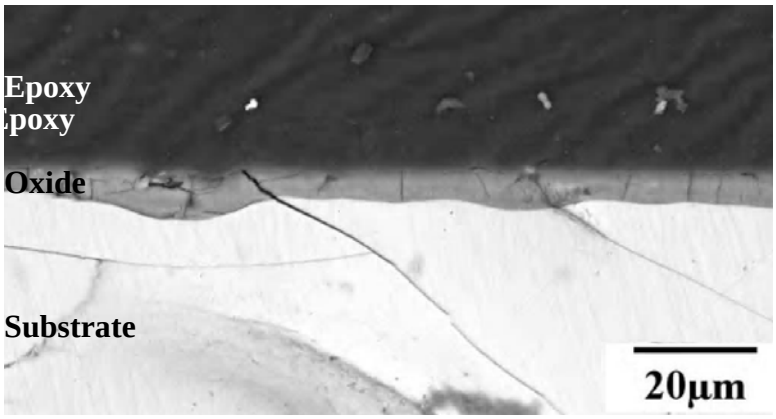

(b)

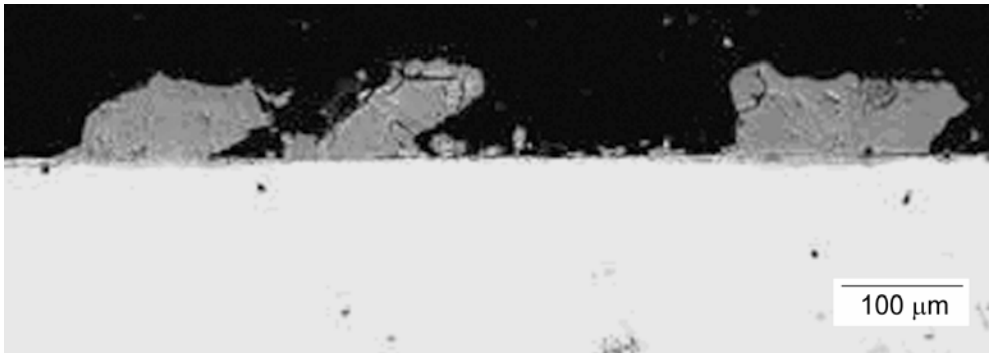

Figure 9. SEM backscatter images of a near surface region of a $Ca_{55}Mg_{15}Al_{10}Zn_{15}Cu_5$ amorphous sample after corrosion in water for 2100 hours. (a) An even oxide layer of about 10 mm thick with cracks stopped at the substrate. (b) High crack frequency shown in both the oxide layer and the substrate. (c) Large globular oxide mounds up to 100 μm thick attached to the first oxide layer.